Scientific Paper / Artículo Científico

UNIVERSIDAD POLITÉCNICA SALESIANA ECUADOR
INGENIUS
Revista de Ciencia y Tecnología
https://doi.org/10.17163/ings.n36.2026.03
pISSN: 1390-650X / eISSN: 1390-860X

# Corrosion inhibition of type N80 carbon steel using eggshell powder in acidic and brine environments: a study based on weight loss testing, micro-indentation, and electrochemical modeling

# Inhibición de la corrosión del acero al carbono tipo N80 utilizando polvo de cáscara de huevo en ambientes ácidos y salinos: un estudio basado en ensayos de pérdida de peso, microindentación y modelado electroquímico

J. L. Dávalos-Monteiro[1,*], C. D. Rodríguez-Hernández[1], R. M. Rached[1], R. Dávalos-Monteiro[2]

Received: 16-10-2025, Received after review: 28-01-2026, Accepted: 21-04-2026, Published: 01-07-2026

## Abstract

Corrosion poses a critical challenge to the oil and gas industry, particularly in systems exposed to acidic and high-salinity environments. This study evaluates eggshell powder, a biowaste-derived material, as a green corrosion inhibitor for type N80 carbon steel under conditions representative of acidic and brine environments. Its performance was systematically assessed through weight loss testing, micro-indentation hardness measurements, and numerical electrochemical modeling. N80 steel coupons were exposed to 2 M hydrochloric acid (HCl) and 2 M sodium chloride (NaCl) solutions, with and without 6 g/L of eggshell powder, for 6 days. Corrosion rates determined from mass loss showed substantial protection in the acidic medium, decreasing from 18.8 to 2.1 mm/year and corresponding to an inhibition efficiency of 90 %. In brine, the effect was more moderate, with a 14% reduction in the corrosion rate. Micro-indentation analysis confirmed that inhibitor-treated samples retained at least 85% of the hardness of unexposed steel in acid, whereas untreated samples exhibited severe mechanical degradation. The results suggest that corrosion protection arises from a combined mechanism involving the formation of a calcium carbonate barrier, stabilization of the corrosion product layer, and possible scavenging of aggressive chloride ions. Overall, this study demonstrates the potential of eggshell powder as a viable and sustainable candidate for corrosion mitigation in harsh industrial environments.

***Keywords***: carbon steel, green corrosion inhibition, eggshell powder, aggressive environments, micro-indentation, sustainability.

## Resumen

La corrosión representa un desafío importante para la industria del petróleo y del gas, especialmente en sistemas expuestos a ambientes ácidos y de alta salinidad. Este estudio evalúa el polvo de cáscara de huevo, un residuo biológico, como inhibidor ecológico de la corrosión del acero al carbono tipo N80 bajo condiciones representativas de ambientes ácidos y salinos. Se analizaron muestras de acero expuestas a soluciones de ácido clorhídrico (HCl) 2 M y cloruro de sodio (NaCl) 2 M, con y sin 6 g/L de polvo de cáscara de huevo, durante seis días. La tasa de corrosión, determinada a partir de la pérdida de masa, mostró una mejora significativa en medio ácido, al disminuir de 18.8 mm/año a 2.1 mm/año, con una eficiencia de inhibición del 90 %. En condiciones salinas, el efecto fue moderado, con una reducción del 14 %. El análisis de microindentación indicó que las muestras tratadas conservaron al menos el 85 % de la dureza del acero no expuesto, mientras que las no tratadas sufrieron una degradación severa. Los resultados sugieren que la protección se debe a la formación de una barrera de carbonato de calcio, la estabilización de la capa de productos de corrosión y la captura de iones agresivos, como el cloruro. Este estudio demuestra que el polvo de cáscara de huevo es una alternativa viable y sostenible para mitigar la corrosión en entornos industriales exigentes.

***Palabras clave***: acero al carbono, inhibidor verde de la corrosión, polvo de cáscara de huevo, ambientes agresivos, microindentación, sustentabilidad

[1,*] Sinopec Tech Middle East LLC, Dhahran 34464-4622, Kingdom of Saudi Arabia.
Corresponding author ✉: jose.stme@sinopec.com.

[2]School of Biological Science and Engineering, Yachay Tech University, Urcuquí, Ecuador.

Suggested citation: J. L. Dávalos-Monteiro, C. D. Rodríguez-Hernández, R. M. Rached and R. Dávalos-Monteiro "Corrosion inhibition of type N80 carbon steel using eggshell powder in acidic and brine environments: a study based on weight loss testing, micro-indentation, and electrochemical modeling," *Ingenius, Revista de Ciencia y Tecnología*, N.° 36, pp. 29-38, 2026, doi: https://doi.org/10.17163/ings.n36.2026.03.

# 1. Introduction

Corrosion is a pervasive degradation process and a critical challenge in multiple engineering applications. In the oil and gas sector, general and localized corrosion commonly occurs in pipelines, storage tanks, and downhole equipment exposed to acidic and high-salinity environments [1–4]. Corrosion compromises equipment structural integrity and can lead to failure, production losses, safety hazards, and significant environmental risks [5–7].

Typical corrosion mitigation strategies and schemes rely on chemical inhibitors based on synthetic organic compounds, such as amines, quaternary ammonium salts, and phosphonates [8–11]. Despite their high efficiency, these inhibitors present several drawbacks, including high cost, limited biodegradability, and environmental toxicity. The need to mitigate corrosion, together with increasing regulatory pressure, has accelerated the search for alternative inhibitors derived from natural or renewable sources, commonly referred to as "green inhibitors" [12, 13].

Green corrosion inhibitors typically include plant extracts, agricultural byproducts, and biowaste materials that are non-toxic, biodegradable, and readily available [14–16]. Eggshells are a notable example, as they are commonly used in the agricultural sector as natural fertilizers. They are primarily composed of calcium carbonate ($CaCO_3$) and organic constituents that may act as corrosion inhibitors by contributing to the formation of a protective film at the metal surface [17–19].

Despite promising early efforts, the use of eggshell-based inhibitors in oil and gas applications remains poorly understood. Previous studies have assessed their performance under model conditions, which differ substantially from highly dynamic field environments where physical and chemical stability must be maintained over extended periods [20, 21]. Therefore, evaluating the degradation of mechanical properties and the durability of the corrosion product layer is critical for assessing the performance of any inhibitor.

Accordingly, this study systematically evaluates the performance of eggshell powder as a corrosion inhibitor under conditions relevant to the oil and gas sector, using both experimental techniques and numerical methods. The N80 steel coupons were exposed to acidic and saline environments, and corrosion rates were determined through weight loss measurements. In addition, micro-indentation analysis was conducted to assess the hardness of the corrosion layers formed with and without the inhibitor. Numerical modeling of corrosion kinetics and inhibitor adsorption provided insight into the possible inhibition mechanism, the effect of eggshell-derived components on anodic and cathodic reactions, and the influence on charge-transfer processes at the steel-electrolyte interface. By combining laboratory experiments with micro-mechanical and numerical analyses, this study assessed the potential of eggshell powder as a green corrosion inhibitor.

# 2. Materials and Methods

## 2.1. Materials

This study used type N80 carbon steel coupons as the metallic substrate for corrosion testing and eggshell powder as the green inhibitor. The chemical composition of the N80 steel, supplied by Changzhou Qingli Huanneng Chemical Technology Co., Ltd., is presented in Table 1. The corrosive media consisted of two aqueous solutions: I) 2 molar sodium chloride (2M NaCl) to simulate saline environments, and II) 2 molar hydrochloric acid (2M HCl) to represent acidic conditions. All chemicals were of analytical grade and were prepared in deionized water (PanReac AppliChem, ITW Reagents).

**Table 1.** Chemical composition of type N80 carbon steel

| Element | Weight (%) |
|---|---|
| Carbon (C) | 0.21 - 0.28 |
| Manganese (Mn) | 0.60 - 1.00 |
| Phosphorus (P) | $\leq$ 0.030 |
| Sulfur (S) | $\leq$ 0.030 |
| Silicon (Si) | 0.15 - 0.35 |
| Chromium (Cr) | $\leq$ 0.25 |
| Nickel (Ni) | $\leq$ 0.25 |
| Copper (Cu) | $\leq$ 0.25 |
| Molybdenum (Mo) | $\leq$ 0.15 |
| Vanadium (V) | $\leq$ 0.08 |
| Other elements | $\leq$ 0.30 (total) |
| Iron (Fe) | Balance |

## 2.2. Sample Preparation

**Steel Coupons & Testing Solutions:**

Type N80 carbon steel plates measuring 50 mm × 10 mm × 3 mm were first ground with No. 50 SiC paper to remove surface oxides and contaminants, ensuring a uniform surface in accordance with ASTM G1. Material removal was controlled to approximately 0.0025 mm in thickness from all surfaces. The samples were then further ground using No. 800 to No. 1200 SiC paper to obtain a suitable surface finish for subsequent testing. After grinding, the coupons were immediately rinsed with deionized water, cleaned with ethanol, and dried with an air gun before initial weighing.

For the test solutions, 116.8 g of NaCl was dissolved and 166.7 ml of concentrated HCl (37%) was diluted in deionized water to obtain 2 M NaCl and 2 M HCl solutions. Their pH values were 7 and 0, respectively.

**Eggshell Inhibitor:**

Eggshells were collected from local sources, thoroughly washed, oven-dried, and ground using a mechanical grinder. The resulting powder was sieved to obtain a uniform particle size corresponding to mesh 80 ($\approx 180\mu m$). Eggshell powder was added to the test solutions at a defined concentration of 6 g/L and mixed until fully dispersed.

### 2.3. Corrosion Testing & Weight Loss Evaluation

Corrosion rates were determined using a classical weight loss protocol. First, each specimen was weighed using an analytical balance with a readability of 1 mg (Mettler Toledo ME203). Then, following ASTM G31, the coupons were placed in glass beakers and immersed in 200 mL of test solution, either 2 M NaCl or 2 M HCl, with or without eggshell inhibitor, for 6 days at room temperature, approximately 23 °C. After exposure, coupons designated for weight loss analysis were removed and gently cleaned in a sonicator bath with deionized water and a soft brush to remove loose corrosion products. Cleaning was omitted for samples intended for micro-indentation to preserve the properties of the corrosion layer. Finally, all coupons were dried with an air gun immediately after cleaning and weighed to three decimal places.

Corrosion rates were calculated using the following equation (1):

$$CR\left[\frac{mm}{year}\right] = \frac{87.6 \cdot (W_i - W_f)}{\rho \cdot A \cdot t} \quad (1)$$

where $W_i$ and $W_f$ are the initial and final masses (mg), $\rho$ is the density of steel ($g/cm^3$), A is the exposed surface area ($cm^2$), and t is the exposure time (hours).

### 2.4. Micro-Indentation Measurements

This study used an instrumented micro-indenter, Anton Paar, Micro Combi Tester MCT, with a maximum load of 30 N, load resolution of 6 $\mu N$, depth range of 1000 $\mu m$, and depth resolution of 0.03 nm, to assess the mechanical properties of the corrosion layer formed on the steel coupons after exposure. The indenter applied several loading and unloading cycles using the continuous multicycle load method, CMC. A matrix of four measurement locations was generated, and the applied force and resulting displacement were recorded. The device measured indentation hardness, HIT, as the mean contact pressure beneath the indenter at peak load, see equation (2):

$$HIT = \frac{F_{max}}{A_p} \quad (2)$$

where $F_{max}$ is the maximum applied load and $A_p$ is the projected contact area, determined using the Oliver-Pharr method. Mean values, standard deviations, and standard errors were reported for each condition to evaluate the integrity and mechanical strength of the protective layer formed in the presence and absence of the inhibitor.

### 2.5. Numerical Simulation

**Electrochemical Corrosion Model Implementation**

The corrosion behavior of type N80 steel was simulated using MATLAB. The numerical model reproduced the electrochemical response of steel in acidic and saline environments with varying solution compositions, inhibitor concentrations, and steel properties. The model incorporated standard corrosion kinetics based on the Butler-Volmer equation and adsorption isotherms to predict current densities and polarization resistance, which are electrochemical parameters related to the corrosion rate.

The simplified model was based on coupled anodic and cathodic reactions described by the Butler-Volmer equation, accounting for charge-transfer kinetics. The general form for each half-cell reaction is:

$$i = i_0 \left( exp\left[\frac{\alpha_a F_\eta}{RT}\right] - exp\left[-\frac{\alpha_c F_\eta}{RT}\right] \right) \quad (3)$$

where $i$ is the current density $A/m^2$; $i_0$ is the exchange current density, $\alpha_a$ and $\alpha_c$ are the anodic and cathodic transfer coefficients, $F$ is Faraday's constant $C/mol$; $\eta$ is the overpotential ($V$), R is the universal gas constant $J/mol \cdot K$; and $T$ is the temperature ($K$).

**Inhibitor Effect via Adsorption Isotherm**

To incorporate the effect of the eggshell inhibitor into the numerical model, the surface coverage ($\theta$) of the inhibitor on the steel surface was estimated using the Langmuir adsorption isotherm [22, 23]. This approach assumes that inhibitor molecules form a layer on the metal surface, with uniform adsorption sites and no interactions between adsorbed species. The surface coverage was calculated as:

$$\theta = \frac{KC}{1 + KC} \quad (4)$$

where $\theta$ is the fraction of the metal surface covered by the inhibitor, $C$ is the inhibitor concentration in $mol \cdot L^{-1}$ and $K$ is the adsorption equilibrium constant in $L \cdot mol^{-1}$. The presence of the inhibitor reduces the active area available for corrosion, and the numerical model accounts for this by scaling the current density from the uninhibited case. Specifically, the corrosion current density in the inhibited system ($i_{corr,inh}$) was estimated as:

$$(i_{corr,inh}) = (1-\theta) i_{corr,uninh} \quad (5)$$

where $i_{corr,uninh}$ is the corrosion current density in the absence of the inhibitor. This formulation allowed the model to account for inhibition efficiency as a function of inhibitor concentration, simulating how increasing surface coverage led to a proportional reduction in electrochemical activity.

**MATLAB Implementation & Numerical Simulation**

The numerical model was developed on MATLAB to simulate the electrochemical behavior of type N80 steel with and without the eggshell inhibitor. The model solves Butler-Volmer equation for both anodic and cathodic reactions across a defined potential range and then adjusts the response based on inhibitor surface coverage.

The simulation started by defining the system parameters, including all constants, electrochemical parameters, and inhibitor properties listed in Table 2. The model then generated a range of electrode potentials around the expected corrosion potential, for example from -0.7 V to -0.3 V, simulating a sweep similar to that used in potentiodynamic polarization experiments [24]. For each potential value, the overpotential $\eta$ was computed and used as the input for the Butler-Volmer equation. Finally, the Butler-Volmer equation was applied to compute the total current density at each potential step. The simulation produced two complete sets of simulated polarization data: one for the uninhibited system and another representing the system with the corrosion inhibitor.

**Table 2.** Parameters used in the numerical corrosion model of type N80 steel in saline (NaCl) and acidic (HCl) systems.

| Parameter | Description | Value NaCl system) | Valor (HCl system) | Unit | Source/Note |
|---|---|---|---|---|---|
| F | Faraday's constant | 96485 | | $C \cdot mol^{-1}$ | Standard constant |
| R | Universal gas constant | 8,314 | | $J \cdot mol^{-1} \cdot K^{-1}$ | Standard constant |
| T | Temperature | 298 | | K | Ambient (25 °C) |
| $\alpha_a$ | Anodic transfer coefficient | 0.5 | | - | Typical assumption |
| $\alpha_c$ | Cathodic transfer coefficient | 0.5 | | - | Typical assumption |
| $i_0$ | Exchange current density | $1 \times 10^{-5}$ | $8 \times 10^{-5}$ | $A \cdot cm^{-2}$ | Estimated for carbon steel in saline water |
| $E_{corr}$ | Corrosion potential | -0.5 | -0.6 | V (vs. Ref) | Estimated |
| K | Adsorption equilibrium constant | 16.28 | 1011 | $L \cdot mol^{-1}$ | Adjusted from experimental data |
| C | Inhibitor concentration | 2 | | $mol \cdot L^{-1}$ | Experimental |
| $\theta$ | Surface coverage | 0.14 | 0.91 | - | From Langmuir isotherm |
| $i_{corr,sin}$ | Corrosion current density (no inhibitor) | $1.56 \times 10^{-5}$ | $1.20 \times 10^{-4}$ | $A/cm^2$ | Model output |
| $i_{corr,con}$ | Corrosion current density (with inhibitor) | $1.34 \times 10^{-5}$ | $1.09 \times 10^{-5}$ | $A/cm^2$ | Model output |

## 3. Results and discussion

### 3.1. Visual Inspection of Corrosion

Figure 1 shows the steel coupons before and after fluid exposure. Visual inspection revealed clear differences in the extent of corrosion between samples exposed to HCl and NaCl solutions. Coupons immersed in HCl exhibited extensive surface degradation, severe rust formation, and visible loss of metallic luster, indicating significant corrosion (Figure 1a). In contrast, coupons exposed to the NaCl solution exhibited more moderate corrosion, with surface discoloration and localized pitting but less widespread material damage than the acid-treated samples (Figure 1b).

A marked protective effect was observed when eggshell powder was added to both solutions. The steel surfaces exposed to the inhibitor exhibited noticeably fewer corrosion products and retained a smoother appearance than the uninhibited controls, as shown in Figure 1. In both acidic and saline environments, the presence of eggshell powder reduced visible corrosion, with the most pronounced effect observed in the HCl solution, where the inhibitor limited the aggressive etching typically seen under these conditions.


(a) (b)

**Figure 1.** N80 Steel coupons images before and after fluid exposure with and without eggshell as an inhibitor. (a) 2 M HCl, (b) 2 M NaCl.

### 3.2. Weight Loss Analysis

Figure 2 presents the corrosion rates of steel coupons with and without the eggshell inhibitor. The corrosion rates estimated after exposure demonstrated the protective effect of the inhibitor. In 2 M NaCl, the corrosion rate without the inhibitor was 0.14 mm/year. The addition of eggshell powder slightly reduced it to 0.12 mm/year, corresponding to an approximately 14% improvement, as shown in Figure 2a. The inhibitor effect was much more pronounced under acidic conditions, in 2 M HCl, where the corrosion rate decreased from 18.8 mm/year without the inhibitor to 2.1 mm/year with the inhibitor, corresponding to an approximately 90% improvement, as shown in Figure 2b.

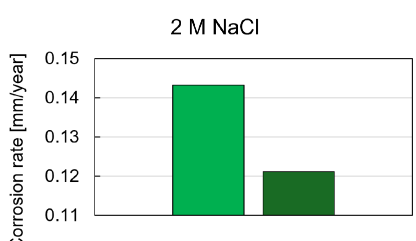


(a)

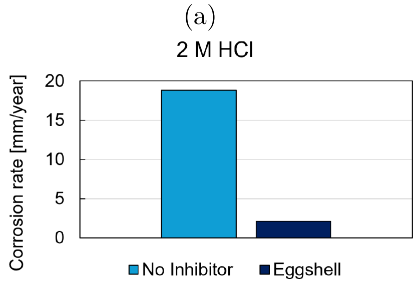


(b)

**Figure 2.** Corrosion rate of N80 carbon steel samples when exposed to a) 2 M NaCl solution and b) 2 M HCl solution with and without eggshell as inhibitor.

These results indicate that eggshell powder provides moderate inhibition in saline environments but substantial protection under highly aggressive acidic conditions. The significant decrease in weight loss in the acid-exposed, inhibitor-treated samples suggests the formation of a protective barrier on the steel, effectively limiting metal dissolution. These findings demonstrate the potential of eggshell-derived inhibitors for corrosion protection in environments where acid exposure is a primary concern, with measurable benefits also observed in brine.

### 3.3. Micro-Indentation Analysis

Figure 3 shows the indentation hardness results for the different coupons. The experimental data indicate that, for samples exposed to 2 M NaCl, hardness values remained similar to those of the unexposed steel, regardless of the presence of the inhibitor, as shown in Figure 3a. The mean HIT changed only from 2.44 GPa for the reference unexposed material to 2.28 GPa without inhibitor and 2.42 GPa with eggshell as the inhibitor, corresponding to a deviation of$\leq$ 7 %. This suggests that, under saline conditions and within the tested exposure time, the surface properties of the steel coupons were minimally affected.

A different trend was observed in acidic environments. Type N80 steel coupons exposed to 2 M HCl without the inhibitor showed a marked decrease in hardness compared with the original unexposed sample, as shown in Figure 3b. HIT decreased to 1.77 GPa in polished coupons to only 0.22 GPa in unpolished coupons. This reduction indicates that the corrosion layer formed in acid was mechanically weak and more susceptible to removal. In contrast, the samples treated with the eggshell inhibitor retained hardness values similar to those of the unexposed material. Polished and unpolished coupons reached 2.07 GPa and 2.32 GPa, respectively, corresponding to at least 85% of the reference value.

The results suggest that the corrosion layer formed in acid without protection was poorly adherent and could be easily removed, leading to continuous exposure of fresh steel to the corrosive fluid and sustained metal loss. When the eggshell inhibitor was added, the resulting layer was mechanically robust and more resistant to removal, effectively serving as a protective barrier. This layer limited further corrosion and enhanced the durability of the steel in service environments exposed to abrasive forces or fluid impingement. Overall, the micro-indentation data support the effectiveness of the eggshell inhibitor in maintaining the mechanical integrity of the steel surface, particularly under aggressive acidic conditions.

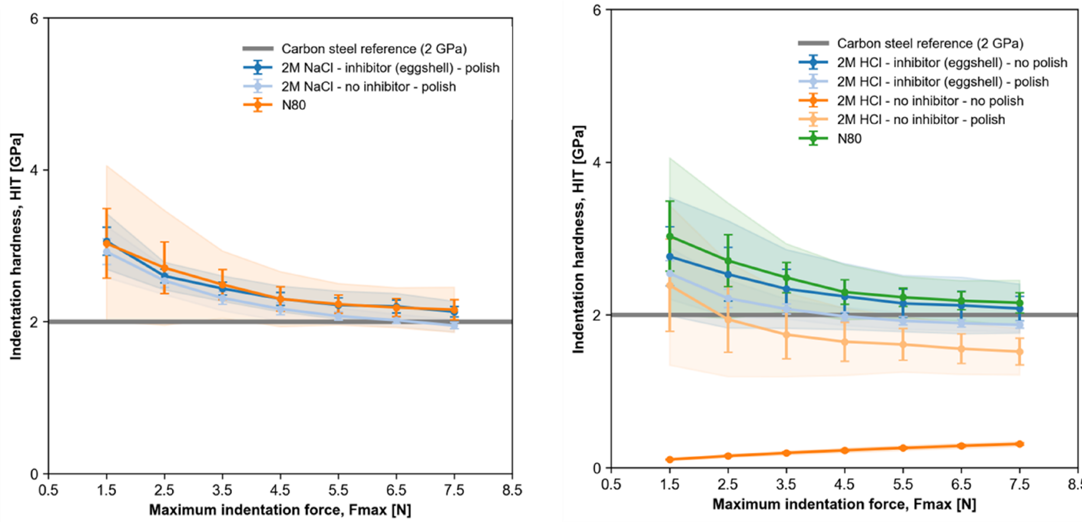


(a) (b)

**Figure 3.** Indentation hardness. a) Brine - 2 M NaCl; b) Acid - 2 M HCl. Note: shaded area shows = −1 standard deviation, bars show ±1 standard error, and data points show mean values.

### 3.4. Numerical Simulation

Figure 4 presents the simulated potentiodynamic polarization curves for the tested solutions with and without the eggshell inhibitor. The simulation revealed differences in corrosion kinetics between neutral chloride and acidic environments. In the 2 M NaCl solution, the current densities were moderate, and the corrosion potential was less negative, consistent with a system in which the cathodic reaction was dominated by oxygen reduction.

The simulated polarization curves for this environment displayed only a minor shift in current density after inhibitor addition, indicating weak surface interaction and limited protective capability, as shown in Figure 4. This behavior was reflected in the inhibition efficiency of only 14%. Based on the simulation results, the uninhibited corrosion current density was approximately $1.56 \times 10^{-5} A/cm^2$, while the inhibited system showed a slight reduction to $1.34 \times 10^{-5} A/cm^2$.

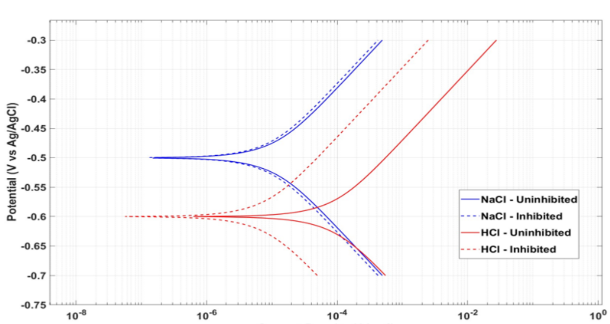


**Figure 4.** Simulated potentiodynamic polarization curves in 2 M NaCl and 2 M HCl with and without the eggshell inhibitor.

In contrast, the numerical results for the 2 M HCl solution showed a much more aggressive corrosive behavior, as expected under acidic conditions favoring hydrogen evolution as the cathodic reaction. The uninhibited system exhibited significantly higher current densities and a more negative corrosion potential, reflecting accelerated anodic dissolution of iron in the steel. However, the addition of eggshell powder at the same acid concentration produced a marked reduction in current density, particularly in the cathodic branch. This behavior was attributed to a higher adsorption constant and near-complete surface coverage, consistent with the experimentally obtained inhibition efficiency of 90%. These results suggest that the acidic environment enhanced the affinity of inhibitor-derived species for the steel surface, possibly through protonation of functional groups or increased chemisorption. Based on the simulation results, the uninhibited corrosion current density in acid was approximately $1.20 \times 10^{-4} A/cm^2$, while the inhibited system showed a marked reduction to $1.09 \times 10^{-5} A/cm^2$.

The differences in corrosion behavior and inhibition efficiency between the two environments demonstrate the role of the medium in controlling the inhibitor performance. Although the same inhibitor concentration was used in both cases, its effectiveness was strongly dependent on electrolyte chemistry. From a modeling perspective, the results validate the usefulness of coupling classical electrochemical kinetics with immersion testing to understand corrosion mechanisms. The Butler–Volmer equation successfully captured the shift in current density profiles, whereas the Langmuir model provided a basis for interpreting the surface interaction between the inhibitor and the substrate. However, the model assumes idealized conditions, such as uniform surface coverage and constant kinetic parameters, which may not fully account for localized corrosion, diffusion effects, or inhibitor degradation. Future work should consider multi-site adsorption models, transport limitations, and pH-dependent speciation to improve predictive accuracy and better reproduce the real systems.

### 3.5. Possible Corrosion Mechanisms & Role of Eggshell as a Corrosion Inhibitor

The deterioration of carbon steel under naturally harsh conditions occurs through spontaneous electrochemical processes at the metal–solution interface. In acid, the carbon steel alloy undergoes anodic dissolution, releasing $Fe^{2+}$ ions, while the cathodic process involves the reduction of hydrogen ions to produce hydrogen gas, commonly known as the hydrogen evolution reaction. In neutral chloride-containing electrolytes, the process is typically less aggressive; however, chloride ions can initiate localized corrosion by disrupting protective films formed at neutral pH, leading to pitting, one of the most critical forms of corrosion because of the difficulty of monitoring it [25].

Eggshell powder is mainly composed of calcium carbonate, along with small amounts of magnesium carbonate, phosphate, and trace organic proteins. Its corrosion protection likely occurs through several simultaneous mechanisms, with the experimental results indicating a stronger inhibitory effect in acidic media. The possible inhibition mechanism in acidic media, based on the experimental data, is described below.

#### Formation of a Carbonate Physical Barrier:

The primary component of eggshell powder, calcium carbonate ($CaCO_3$), can form a protective barrier on the steel surface. In acidic environments such as 2 M HCl, calcium carbonate reacts with $H^+$ to release soluble $Ca^{2+}$ ions and carbon dioxide gas ($CO_2$). The reaction proceeds as follows:

$$CaCO_3(s)+2H^+(aq) \rightarrow Ca^{2+}(aq)+CO_2(g)+H_2O(l) \quad (6)$$

Once $Ca^{2+}$ is released into solution, it can reprecipitate near the metal surface, particularly under localized conditions where pH increases due to cathodic reactions such as hydrogen evolution, which consumes $H^+$:

$$2H^+(aq) + 2e^- \rightarrow H_2(g) \quad (7)$$

In these alkaline areas, $Ca^{2+}$ can react with carbonate ions (${CO_3}^{2-}$) or hydroxide ions ($OH^-$) to reform calcium carbonate or produce calcium hydroxide, also known as portlandite. Both compounds are poorly soluble and can form solid deposits on the steel surface. These two reactions can proceed as follows:

$$Ca^{2+} + CO_3^{2-} \rightarrow CaCO_3(s) \quad (8)$$

$$Ca^{2+} + 2OH^- \rightarrow Ca(OH)_2(s) \quad (9)$$

The precipitated compounds from reactions (8) and (9), particularly calcium carbonate ($CaCO_3$), can form a compact layer on the steel surface that acts as a barrier. This physical barrier reduces the transport of aggressive ions, such as chloride ($Cl^-$) and hydrogen ions ($H^+$), by slowing or limiting their diffusion toward the metal surface. As a result, it restricts anodic dissolution by partially blocking active corrosion sites, thereby decreasing the electroactive area and slowing the corrosion rate. Figure 5 presents a schematic of the proposed physical barrier formation mechanism.

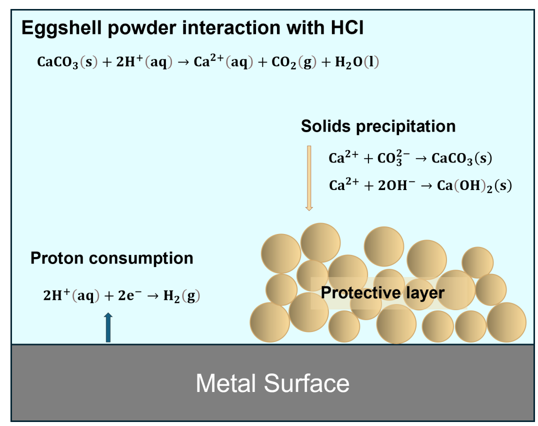


**Figure 5.** Schematic of calcium carbonate physical barrier formation on the steel surface.

#### Modification of the Corrosion Product Layer:

The addition of eggshell components may alter the structure and properties of the corrosion product layer, making it more stable, denser, and less prone to cracking or detachment. This is consistent with the increased surface hardness observed in the presence of the inhibitor, particularly in acid. A mechanically stable layer resists detachment caused by flow or abrasion, thereby decreasing the likelihood of further exposure and metal loss.

#### Potential Scavenging of corrosion aggressive Ions:

Calcium ions released from eggshell powder may interact with free chloride ions in solution, reducing their activity and helping prevent localized attack, such as pitting.

Corrosion inhibition through a scavenging mechanism may have contributed specifically to the brine experiment, where the high concentration of chloride ions likely interacted with calcium ions released from the eggshell powder. Once aggressive anions are scavenged, their ability to disrupt passive films or initiate localized corrosion is reduced. In addition, excess $Ca^{2+}$ in solution may lead to the formation of slightly soluble calcium species, such as calcium chloride complexes or calcium carbonate, depending on pH and carbonate availability. Figure 6 illustrates the corrosion inhibition mechanism involving chloride ions and calcium ions acting as scavengers.

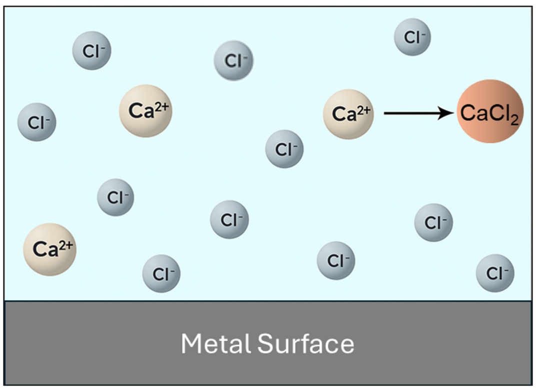


**Figure 6.** Corrosion inhibition through a scavenging mechanism of Chloride ions by Calcium ions.

In summary, the combined effects of barrier formation and modification of the corrosion product layer may account for the effective inhibition performance of eggshell powder, particularly under acidic conditions. By forming a more protective and mechanically stable surface film, eggshell-derived inhibitors can help preserve steel integrity and slow corrosion progression, supporting their potential application as a green corrosion inhibition strategy in harsh environments.

## 4. Conclusions

The results of this experimental study demonstrate that eggshell powder effectively inhibits the corrosion of type N80 carbon steel, particularly under aggressive acidic conditions. The notable reduction in corrosion rate, supported by weight loss measurements, indicates that eggshell powder substantially reduces metal dissolution in 2 M HCl, achieving an inhibition efficiency of 90%. This is an important finding, as acidic environments pose a major challenge in several field operations.

Micro-indentation analysis revealed negligible hardness changes in brine, with values of 2.44 GPa for unexposed steel, 2.28 GPa without the inhibitor, and 2.42 GPa with eggshell powder. In contrast, exposure to 2 M HCl without protection reduced surface hardness to 1.77 GPa in polished coupons and 0.22 GPa in unpolished coupons. This low hardness indicates the formation of a weak, poorly adherent corrosion layer that can be removed easily, continually exposing fresh steel to acid attack. The addition of eggshell powder increased hardness to 2.07 and 2.32 GPa, confirming the formation of a dense, well-bonded film that resisted removal, limited further corrosion, and improved durability under abrasive or high-flow conditions.

The numerical simulation, which incorporated Butler-Volmer kinetics and Langmuir adsorption isotherms, reproduced the distinct behaviors observed experimentally in both saline and acidic systems. The agreement between simulated and experimental data highlights the value of combining experimental techniques with numerical analysis to understand and propose possible corrosion mechanisms.

Overall, the coupled effects of barrier formation, corrosion product stabilization, and chloride ion scavenging collectively contributed to the inhibition performance of eggshell powder. These findings position eggshell powder as a viable candidate for future application in corrosion control strategies for harsh industrial environments.

## Contributor Roles

- **J. L. Dávalos-Monteiro:** Conceptualization, research, methodology, formal analysis, writing – original draft, writing – revision and editing.
- **C. D. Rodríguez-Hernández:** Conceptualization, research, methodology, formal analysis, writing – original draft, writing – revision and editing.
- **R. M. Rached:** Conceptualization, research, methodology, formal analysis, writing – original draft, writing – revision and editing.
- **R. Dávalos-Monteiro:** Conceptualization, research, methodology, formal analysis, writing – original draft, writing – revision and editing, supervision.

## References

[1] M. Kermani and A. Morshed, "Carbon dioxide corrosion in oil and gas production—a compendium," *Corrosion*, vol. 59, no. 8, pp. 659–683, Aug. 2003. [Online]. Available: https://doi.org/10.5006/1.3277596

[2] Y. T. Al-Janabi, "An overview of corrosion in oil and gas industry: Upstream, midstream, and downstream sectors," *Corrosion Inhibitors in the Oil and Gas Industry*, pp. 1–39, Feb. 2020. [Online]. Available: https://doi.org/10.1002/9783527822140.ch1

[3] S. Papavinasam, *Corrosion control in the oil and gas industry.* Elsevier, 2014. [Online]. Available: https://doi.org/10.1016/C2011-0-04629-X

[4] G. M. Castro, J. Park, A. Sherik, and J. C. Santamarina, "Metal corrosion in partially saturated sands: pore fluid conductivity and water saturation," *Canadian Geotechnical Journal*, vol. 62, pp. 1–13, Jan. 2025. [Online]. Available: https://doi.org/10.1139/cgj-2024-0097

[5] R. B. Jackson, "The integrity of oil and gas wells," *Proceedings of the National Academy of Sciences*, vol. 111, no. 30, pp. 10 902–10 903, 2014. [Online]. Available: https://doi.org/10.1073/pnas.1410786111

[6] A. A. Soomro, A. A. Mokhtar, J. C. Kurnia, N. Lashari, H. Lu, and C. Sambo, "Integrity assessment of corroded oil and gas pipelines using machine learning: A systematic review," *Engineering Failure Analysis*, vol. 131, p. 105810, Jan. 2022. [Online]. Available: https://doi.org/10.1016/j.engfailanal.2021.105810

[7] O. Shabarchin and S. Tesfamariam, "Internal corrosion hazard assessment of oil & gas pipelines using bayesian belief network model," *Journal of Loss Prevention in the Process Industries*, vol. 40, pp. 479–495, Mar. 2016. [Online]. Available: https://doi.org/10.1016/j.jlp.2016.02.001

[8] G. Camila and F. Alexandre, *Corrosion Inhibitors – Principles, Mechanisms and Applications*. InTech, Feb. 2014. [Online]. Available: https://doi.org/10.5772/57255

[9] P. B. Raja, M. Ismail, S. Ghoreishiamiri, J. Mirza, M. C. Ismail, S. Kakooei, and A. A. Rahim, "Reviews on corrosion inhibitors: A short view," *Chemical Engineering Communications*, vol. 203, no. 9, pp. 1145–1156, 2016. [Online]. Available: https://doi.org/10.1080/00986445.2016.1172485

[10] V. S. Sastri, *Corrosion Inhibitors: Principles and Application*. Wiley, 1998. [Online]. Available: https://upsalesiana.ec/ing36ar3r10

[11] A. Kadhum, A. A. Al-Amiery, R. Alazawi, M. K. S. Al-Ghezi, and R. H. Abass, "Corrosion inhibitors. A review," *International Journal of Corrosion and Scale Inhibition*, vol. 10, no. 1, Mar. 2021. [Online]. Available: https://doi.org/10.17675/2305-6894-2021-10-1-3

[12] V. S. Sastri, *Green Corrosion Inhibitors: Theory and Practice*. Wiley, May 2011. [Online]. Available: http://doi.org/10.1002/9781118015438

[13] L. T. Popoola, "Organic green corrosion inhibitors (OGCIs): a critical review," *Corrosion Reviews*, vol. 37, no. 2, pp. 71–102, Jan. 2019. [Online]. Available: https://doi.org/10.1515/corrrev-2018-0058

[14] N. Hossain, M. Asaduzzaman Chowdhury, and M. Kchaou, "An overview of green corrosion inhibitors for sustainable and environment friendly industrial development," *Journal of Adhesion Science and Technology*, vol. 35, no. 7, pp. 673–690, 2020. [Online]. Available: https://doi.org/10.1080/01694243.2020.1816793

[15] A. Miralrio and A. Espinoza Vázquez, "Plant extracts as green corrosion inhibitors for different metal surfaces and corrosive media: A review," *Processes*, vol. 8, no. 8, p. 942, Aug. 2020. [Online]. Available: https://doi.org/10.3390/pr8080942

[16] S. Marzorati, L. Verotta, and S. P. Trasatti, "Green corrosion inhibitors from natural sources and biomass wastes," *Molecules*, vol. 24, no. 1, p. 48, Dec. 2018. [Online]. Available: https://doi.org/10.3390/molecules24010048

[17] M. Alfattah, I. G. A. Arwati, Arramel, A. A. Afkauni, and R. M. Yofatama, "Efficiency of eggshell waste as a metal corrosion inhibitor ss316l based on green technology in seawater media," *Journal of Physics: Conference Series*, vol. 2942, no. 1, p. 012017, Feb. 2025. [Online]. Available: https://doi.org/10.1088/1742-6596/2942/1/012017

[18] O. Sanni, A. Popoola, and O. Fayomi, "The inhibitive study of egg shell powder on uns n08904 austenitic stainless steel corrosion in chloride solution," *Defence Technology*, vol. 14, no. 5, pp. 463–468, Oct. 2018. [Online]. Available: https://doi.org/10.1016/j.dt.2018.07.015

[19] V. S. Aigbodion and E. Dinneya-Onuoha, "Unveiling the anti-corrosion properties of Zn-eggshell particle composite coatings on mild steel in seawater-simulated solution using starch as a modifier," *RSC Advances*, vol. 14, no. 34, pp. 24 548–24 560, 2024. [Online]. Available: https://doi.org/10.1039/d4ra04283b

[20] O. Sanni, S. A. Iwarere, and M. O. Daramola, "Investigation of eggshell agro-industrial waste as a potential corrosion inhibitor for mild steel in oil and gas industry," *Sustainability*, vol. 15, no. 7, p. 6155, Apr. 2023. [Online]. Available: https://doi.org/10.3390/su15076155

[21] S. K. Alias, H. F. Pahroraji, H. M. Hairi, M. M. Ali, M. A. M. Shah, and B. Abdullah, "Eggshell waste extract as potential natural corrosion inhibitor for AISI 1020 steel in acidic environment," *Journal of Mechanical Engineering and Sciences*, pp. 10 192–10 201, 2024. [Online]. Available: https://doi.org/10.15282/jmes.18.3.2024.8.0805

[22] A. Kokalj, "On the use of the langmuir and other adsorption isotherms in corrosion inhibition," *Corrosion Science*, vol. 217, p. 111112, 2023. [Online]. Available: https://doi.org/10.1016/j.corsci.2023.111112

[23] E. Ituen, O. Akaranta, and A. James, "Evaluation of performance of corrosion inhibitors using adsorption isotherm models: An overview," *Chemical Science International Journal*, vol. 18, no. 1, pp. 1–34, Jan. 2017. [Online]. Available: https://doi.org/10.9734/CSJI/2017/28976

[24] R. Dávalos Monteiro, J. van de Wetering, B. Krawczyk, and D. L. Engelberg, "Corrosion behaviour of type 316l stainless steel in hot caustic aqueous environments," *Metals and Materials International*, vol. 26, no. 5, pp. 630–640, Oct. 2019. [Online]. Available: https://doi.org/10.1007/s12540-019-00403-2

[25] R. L. Dávalos Monteiro and S. D. Ananda, "Pitting corrosion of type 304 stainless steel and sulfate inhibition effect in chloride containing environments," *Revista Tecnológica - ESPOL*, vol. 30, no. 3, 2017. [Online]. Available: https://upsalesiana.ec/ing36ar3r25